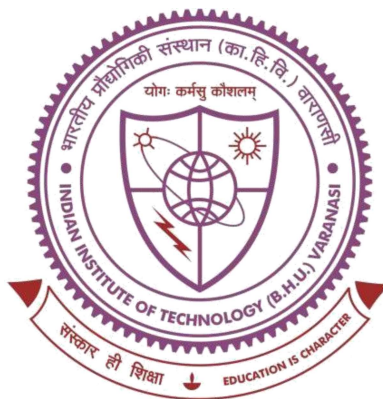


**Tracing the Anti-Cancer Mechanism of *Pleurotus osteratus*
Fractionate *via* Integrated Strategy of Network
Pharmacology and Experimental Studies**



**Thesis submitted in partial fulfilment
for the Award of Degree**

Doctor of Philosophy

By

Singh Shreya Hariawadhsingh

**DEPARTMENT OF PHARMACEUTICAL
ENGINEERING & TECHNOLOGY
INDIAN INSTITUTE OF TECHNOLOGY
(BANARAS HINDU UNIVERSITY)
VARANASI – 221005**

Roll No. 16161503

2022

CERTIFICATE

It is certified that the work contained in the thesis titled “*Tracing the Anti-Cancer Mechanism of Pleurotus osteratus Fractionate via Integrated Strategy of Network Pharmacology and Experimental Studies*” by *Mrs. Singh Shreya Hariawadhsingh* has been carried out under my supervision and that this work has not been submitted elsewhere for a degree.

It is further certified that the student has fulfilled all the requirements of Comprehensive Examination, Candidacy and SOTA for the award of Ph.D. degree.

Dr. Alakh N. Sahu
Supervisor

DECLARATION BY THE CANDIDATE

I, "***Singh Shreya Hariawadhsingh***", certify that the work embodied in this thesis is my own bonafide work and carried out by me under the supervision of "***Dr. Alakh N. Sahu***" from "***January 2017***" to "***December 2022***", at the "***Department of Pharmaceutical Engineering & Technology***", Indian Institute of Technology (BHU), Varanasi. The matter embodied in this thesis has not been submitted for the award of any other degree/diploma. I declare that I have faithfully acknowledged and given credits to the research workers wherever their works have been cited in my work in this thesis. I further declare that I have not willfully copied any other's work, paragraphs, text, data, results, etc., reported in journals, books, magazines, reports dissertations, theses, *etc.*, or available at websites and have not included them in this thesis and have not cited as my own work.

Date: 30 December 2022

Place: Varanasi

Singh Shreya Hariawadhsingh

CERTIFICATE BY THE SUPERVISOR

It is certified that the above statement made by the student is correct to the best of my knowledge.

Dr. Alakh N. Sahu
Supervisor

Prof. S. Hemalatha
Head of the Department

COPYRIGHT TRANSFER CERTIFICATE

Title of the Thesis: Tracing the Anti-Cancer Mechanism of *Pleurotus osteratus* Fractionate via Integrated Strategy of Network Pharmacology and Experimental Studies

Name of the Student: Singh Shreya Hariawadhsingh

Copyright Transfer

The undersigned hereby assigns to the Indian Institute of Technology (Banaras Hindu University), Varanasi, all rights under copyright that may exist in and for the above thesis submitted for the award of the *“Doctor of Philosophy”*.

Date: 30 December 2022

Singh Shreya Hariawadhsingh

Place: Varanasi

Note: However, the author may reproduce or authorize others to reproduce material extracted verbatim from the thesis or derivative of the thesis for author's personal use provided that the source and the Institute's copyright notice are indicated.

Acknowledgement

I would like to thank the *Ganapati Bappa* for showering his continuous blessings, *Bharat Ratna Mahamana Pandit Madan Mohan Malviya ji*, and *M L Shroff* for establishing the glorious temple of learning.

I would like to express profound gratitude and indebtedness to my venerated mentor and supervisor *Dr. Alakh N Sahu*, for his patience, motivation, and immense support. His guidance enabled me to complete my research work smoothly.

I am deeply thankful to *Prof Hemalatha Siva*, Head, Department of Pharmaceutical Engineering & Technology, IIT (BHU), Varanasi for providing moral support and research facilities for my research work.

I am immensely thankful to all former Head of the Department *Prof. B. Mishra*, *Prof. S. K. Singh*, *Prof Sanjay Singh*, and *Prof. S. K. Shrivastava* for their cooperation during my research work.

I wish to express deep regard to all the faculty member (*Prof. S. Krishnamurthy*, *Dr. Senthil Raja A.*, *Dr. Ruchi Chawla*, *Dr. M. S. Muthu*, *Dr. Gyan Prakash Modi*, *Dr. Vinod Tiwari*, *Dr. Sunil Kumar Mishra*, *Dr. Prasanta Kumar Nayak*, *Dr. Shreyans Kumar Jain*, *Dr. Ashish Kumar Agrawal*, *Dr. Rajnish*, *Dr. Deepak Kumar*, *Dr. Dinesh Kumar*, *Dr. Jairam Meena*, *Dr. Ashok Kumar*, and *Dr. Arun Khatri*) of Department for their co-operation and suggestion during my research work.

I am obliged to all *RPEC members* for providing valuable suggestions in my research work.

I am also thankful to our *Departmental staff* for their cooperation and support.

I am thankful to *Dr. Deepak Kasote*, IRRI (South-Asia), *Dr. Santosh Guru*, NIPER (Hyderabad), and *Dr. Ashish Kumar Aggarwal* for their collaborative work.

My heartiest thanks to my batch mates, juniors, and seniors, *Debadatta, Sangeetha, Ojaswi, Shivani, Gaurav, Naveen, Deepa, Aiswarya, Rohit, Abhishek, Dubey, Bhanu, Vineeta (ma'am), Qadir, Rama, Prabha, Bikash, Sagar, Himani, Reena, Pooja* and *Pradeep* for their care & moral support.

Ministry of Human Resource and Development (MHRD), New Delhi is gratefully acknowledged for providing fellowship during the tenure of my research work.

No words can describe how I am thankful to my family: *father, mother, brother, husband, Mansi (ma'am), Aditi, Anandi, Rajveer*, and my *in-laws*.

At last to my strength and weakness, my five and half year-old daughter '*Saanvi*'.

Table of contents

| | |
|--|-------|
| List of Figures | xii |
| List of Tables | xvi |
| List of Equations | xviii |
| Symbols | xix |
| Preface | xxiii |
| Chapter 1. Introduction | 26 |
| 1.1. Overview of <i>Pleurotus</i> mushroom | 26 |
| 1.1.1. Mushroom: A historical journey from ‘culinary delicacy’ to ‘medicinal value’ | 26 |
| 1.1.2. <i>Pleurotus</i> mushroom..... | 27 |
| 1.1.3. Anti-cancer potential of <i>Pleurotus</i> mushroom..... | 29 |
| 1.1.4. Anti-cancer potential bioactive myco-metabolites from <i>Pleurotus</i> mushroom | 35 |
| 1.1.4.1. Higher molecular weight bioactive myco-metabolites..... | 35 |
| 1.1.4.2. Lower molecular weight bioactive myco-metabolites | 36 |
| 1.1.5. Explored mechanistic pathway for anti-cancer potential of <i>Pleurotus</i> mushroom | 37 |
| 1.2. Overview of chemometric | 39 |
| 1.3. Overview of network pharmacology | 39 |
| 1.4. Rationale & Objectives..... | 41 |
| Chapter 2. Bioactivity-based screening of different species of <i>Pleurotus</i> mushroom with their myco-chemical profiling | 44 |
| 2.1. Background..... | 44 |
| 2.2. Objectives | 46 |
| 2.3. Experimental work | 46 |
| 2.3.1. Material, Chemicals, and Reagents | 46 |
| 2.3.2. Extraction..... | 47 |
| 2.3.3. Qualitative myco-chemical analysis..... | 48 |
| 2.3.4. Quantitative myco-chemical analysis..... | 48 |
| 2.3.4.1. Estimation of total phenolics | 48 |
| 2.3.4.2. Estimation of total flavonoids | 48 |
| 2.3.4.3. Estimation of total protein content | 48 |

| | | |
|---|---|----|
| 2.3.4.4. | Estimation of total carbohydrates content | 49 |
| 2.3.5. | <i>In-vitro</i> cytotoxic activity | 49 |
| 2.3.6. | <i>In-vitro</i> free radical scavenging activity | 50 |
| 2.3.6.1. | DPPH assay..... | 50 |
| 2.3.6.2. | ABTS ⁺ assay..... | 50 |
| 2.3.7. | HPTLC-based method development, validation, and quantification of ergosterol content..... | 51 |
| 2.3.7.1. | Preparation of standard and sample solution | 51 |
| 2.3.7.2. | Chromatographic operative condition | 51 |
| 2.3.7.3. | Method validation..... | 52 |
| 2.3.7.3.1. | Calibration curve | 52 |
| 2.3.7.3.2. | Specificity | 52 |
| 2.3.7.3.3. | Sensitivity | 52 |
| 2.3.7.3.4. | Precision..... | 52 |
| 2.3.7.3.5. | Accuracy | 53 |
| 2.3.7.4. | Quantification of ergosterol in the crude extract..... | 53 |
| 2.4. | Results and discussion | 53 |
| 2.4.1. | Extraction yield | 53 |
| 2.4.2. | Qualitative myco-chemical analysis..... | 54 |
| 2.4.3. | Quantitative myco-chemical analysis..... | 54 |
| 2.4.4. | <i>In-vitro</i> cytotoxic activity | 56 |
| 2.4.5. | <i>In-vitro</i> free radical scavenging activity | 58 |
| 2.4.6. | HPTLC-based method development, validation, and quantification of ergosterol content..... | 62 |
| 2.5. | Summary..... | 67 |
| Chapter 3. Chemometric-based analysis of myco-metabolite of bioactive enriched fraction of <i>Pleurotus osteratus</i> and its correlation with <i>in-vitro</i> cytotoxic activity.... | | 69 |
| 3.1. | Background | 69 |
| 3.2. | Objectives | 70 |
| 3.3. | Experimental work | 70 |
| 3.3.1. | Material, Chemicals, and Reagents | 70 |
| 3.3.2. | Authentication..... | 70 |
| 3.3.2.1. | Molecular characterization..... | 70 |
| 3.3.2.2. | Taxonomical characterization | 71 |
| 3.3.3. | Bioassay guided fractionation..... | 72 |
| 3.3.4. | <i>In-vitro</i> cytotoxic activity | 72 |

| | | |
|------------|---|-----|
| 3.3.5. | LC-MS/MS-based quantitative profiling of phenolic acids, flavonoids, and ergosterol | 73 |
| 3.3.6. | LC-QTOF/MS-based untargeted myco-metabolite profiling | 74 |
| 3.3.7. | Chemometric analysis | 75 |
| 3.3.8. | Headspace Gas Chromatography (GC-HS) based solvent residual analysis | 75 |
| 3.4. | Result and discussion | 75 |
| 3.4.1. | Authentication | 75 |
| 3.4.1.1. | Molecular characterization | 75 |
| 3.4.1.2. | Taxonomical characterization | 77 |
| 3.4.2. | <i>In-vitro</i> cytotoxic activity | 79 |
| 3.4.3. | LC-MS/MS-based quantitative profiling of phenolic acids, flavonoids, and ergosterol | 82 |
| 3.4.4. | LC-QTOF/MS-based untargeted myco-metabolite profiling | 84 |
| 3.4.5. | Chemometric analysis | 90 |
| 3.4.6. | Headspace Gas Chromatography (GC-HS) based solvent residual analysis | 95 |
| 3.5. | Summary | 95 |
| Chapter 4. | Tracing the anti-cancer mechanism of HFPO1 by the integrative approach of network pharmacology and experimental studies | 98 |
| 4.1. | Background | 98 |
| 4.2. | Objectives | 99 |
| 4.3. | Experimental work | 99 |
| 4.3.1. | Preliminary work | 99 |
| 4.3.2. | Network pharmacology | 100 |
| 4.3.2.1. | <i>In-silico</i> drug-likeness screening | 100 |
| 4.3.2.2. | Compound-target prediction | 100 |
| 4.3.2.3. | Diseases-target prediction | 100 |
| 4.3.2.4. | Protein-protein interaction | 101 |
| 4.3.2.5. | Gene enrichment analysis | 101 |
| 4.3.2.6. | Network layout of compound-target | 102 |
| 4.3.2.7. | <i>In-silico</i> molecular docking | 102 |
| 4.3.2.8. | <i>In-silico</i> cancer multi-omics expression study & prognostic potential .. | 103 |
| 4.3.3. | <i>In-vitro</i> experimental validation | 104 |
| 4.3.3.1. | Fluorescence microscopy | 104 |
| 4.3.3.2. | Immunoblot analysis | 104 |

| | | |
|---|---|-----|
| 4.3.4. | <i>In-vivo</i> experimentation | 105 |
| 4.3.4.1. | Experimental animals | 105 |
| 4.3.4.2. | Acute toxicity assessment | 105 |
| 4.3.5. | <i>In-vivo</i> anti-tumor efficacy in EAC (solid tumor) bearing Swiss albino mice | 106 |
| 4.4. | Results and Discussion | 109 |
| 4.4.1. | Network pharmacology | 109 |
| 4.4.1.1. | <i>In-silico</i> drug-likeness screening | 109 |
| 4.4.1.2. | Compound-target prediction | 109 |
| 4.4.1.3. | Diseases-target prediction | 113 |
| 4.4.1.4. | Protein-protein interaction | 120 |
| 4.4.1.5. | Gene enrichment analysis | 124 |
| 4.4.1.6. | Network layout of compound-target | 126 |
| 4.4.1.7. | <i>In-silico</i> docking interaction of hub targets and key myco-metabolites .. | 129 |
| 4.4.1.8. | <i>In-silico</i> cancer multi-omics expression study & prognostic potential .. | 131 |
| 4.4.2. | <i>In-vitro</i> experimental validation | 132 |
| 4.4.2.1. | Fluorescence microscopy | 132 |
| 4.4.2.2. | Immunoblot analysis | 134 |
| 4.4.3. | <i>In-vivo</i> experimentation | 135 |
| 4.4.3.1. | Acute toxicity assessment | 135 |
| 4.4.3.2. | <i>In-vivo</i> anti-tumor efficacy in EAC (solid tumor) bearing Swiss albino mice | 137 |
| 4.5. | Summary | 140 |
| Chapter 5. Tracing the anti-cancer mechanism of EFPO1 by the integrative approach of network pharmacology and experimental studies..... | | 146 |
| 5.1. | Background | 146 |
| 5.2. | Objectives | 147 |
| 5.3. | Experimental work | 147 |
| 5.3.1. | Preliminary work..... | 147 |
| 5.3.2. | Network pharmacology | 148 |
| 5.3.2.1. | <i>In-silico</i> drug-likeness screening | 148 |
| 5.3.2.2. | Compound-target prediction | 148 |
| 5.3.2.3. | Diseases-target prediction | 148 |
| 5.3.2.4. | Protein-protein interaction | 149 |
| 5.3.2.5. | Gene enrichment analysis | 149 |
| 5.3.2.6. | Network layout of compound-target | 149 |

| | | |
|------------|--|-----|
| 5.3.2.7. | <i>In-silico</i> molecular docking | 149 |
| 5.3.2.8. | <i>In-silico</i> cancer multi-omic expression study & prognostic potential.... | 150 |
| 5.3.3. | In-vitro experimental validation..... | 150 |
| 5.3.3.1. | Fluorescence microscopy..... | 150 |
| 5.3.3.2. | Immunoblot analysis | 150 |
| 5.3.4. | <i>In-vivo</i> experimentation..... | 150 |
| 5.3.4.1. | Experimental animals | 150 |
| 5.3.4.2. | Acute toxicity assessment..... | 151 |
| 5.3.5. | In-vivo anti-tumor efficacy in EAC (solid tumor) bearing Swiss albino mice | 151 |
| 5.4. | Results and Discussion | 151 |
| 5.4.1. | Network pharmacology | 151 |
| 5.4.1.1. | <i>In-silico</i> drug-likeness screening..... | 151 |
| 5.4.1.2. | Compound-target prediction | 152 |
| 5.4.1.3. | Diseases-target prediction..... | 156 |
| 5.4.1.4. | Protein-protein interaction | 164 |
| 5.4.1.5. | Gene enrichment analysis | 168 |
| 5.4.1.6. | Network layout of compound-target | 170 |
| 5.4.1.7. | <i>In-silico</i> docking interaction of hub targets and key myco-metabolites. | 173 |
| 5.4.1.8. | <i>In-silico</i> cancer multi-omic expression study & prognostic potential of selected hub target..... | 175 |
| 5.4.2. | <i>In-vitro</i> experimental validation..... | 176 |
| 5.4.2.1. | Fluorescence microscopy..... | 176 |
| 5.4.2.2. | Immunoblot analysis | 177 |
| 5.4.3. | <i>In-vivo</i> experimentation..... | 178 |
| 5.4.3.1. | Acute toxicity assessment..... | 178 |
| 5.4.3.2. | <i>In-vivo</i> anti-tumor efficacy in EAC (solid tumor) bearing Swiss albino mice | 180 |
| 5.5. | Summary..... | 183 |
| Chapter 6. | Summary and Conclusion | 187 |
| | Reference and Bibliography | 191 |
| | <i>Appendix</i> | 204 |
| | Publication..... | 211 |

List of Figures

| | |
|--|----|
| Figure 1.1. Schematic diagram of <i>Pleurotus</i> mushroom..... | 28 |
| Figure 1.2. Explored lower molecular weight myco-metabolites for anti-cancer potential of <i>Pleurotus</i> mushroom..... | 37 |
| Figure 1.3. Explored mechanistic pathway involved in the anti-cancer potential of <i>Pleurotus</i> mushroom. Red circles are the explored mechanism. Modified image of Kyoto Encyclopedia of Genes and Genomes (KEGG) pathway of cancer. | 38 |
| Figure 2.1. Schematic representation of extraction procedure. | 47 |
| Figure 2.2. Calibration curve of the standard compound (a) gallic acid (10-50 µg/mL), (b) quercetin (2-10 µg/mL), (c) d-glucose (20-100 µg/mL), and (d) BSA (62.5-100 µg/mL)..... | 55 |
| Figure 2.3. <i>In-vitro</i> cytotoxic activity of DCM: Et and hydroalcoholic crude extract against (a) MDA-MB-231, (b) B16F10, and (c) HEK-293 cell line. Non-linear regression analysis was performed for the determination of IC ₅₀ . Values are expressed as mean ± SD of three parallel measurements. One-way ANOVA was performed, followed by a turkey's multiple comparison test using Graph pad prism 5.0. Different letters (a, b, c, d, e, f, g, h, i, and j) represent a significant difference (p < 0.05), and the same letter indicates the absence of a significant difference between the results..... | 57 |
| Figure 2.4. DPPH scavenging potential of DCM:Et crude extract and hydroalcoholic crude extract (a) PO1 (b) PE1 (c) PF1 (d) PS1 (e) PD1, (f) PO2 (g) PE2 (h) PF2 (i) PS2 and (j) PD2..... | 60 |
| Figure 2.5. ABTS ⁺ Scavenging potential of DCM:Et crude extract and hydroalcoholic crude extract (a) PO1 (b) PE1 (c) PF1 (d) PS1 and (e) PD1, (f) PO2 (g) PE2 (h) PF2 (i) PS2 and (j) PD2. | 61 |
| Figure 2.6. <i>In-vitro</i> free radical scavenging activity of DCM: Et and hydroalcoholic crude extract against (a) DPPH radical with inset figure of ascorbic acid, and (b) ABTS ⁺ radical with inset figure of trolox..... | 62 |
| Figure 2.7. Calibration curve and densitometric chromatogram of standard ergosterol with DCM: Et crude extract (a) Calibration curve of standard ergosterol mean peak area versus concentration (µg/spot) (n = 3) (b) 3-D Overlay λ _{max} spectra of standard ergosterol with DCM: Et crude extract at 283 nm, and (c) 3-D Densitometric chromatogram of standard ergosterol with DCM: Et crude extract at 283 nm. | 63 |
| Figure 2.8. HPTLC fingerprinting of standard ergosterol with DCM: Et crude extract (a) captured at 256 nm, and (b) captured at 366 nm. | 64 |
| Figure 2.9. Densitometric chromatogram and HPTLC fingerprinting of standard ergosterol with hydroalcoholic crude extract (a) 3-D Densitometric chromatogram of standard ergosterol with hydroalcoholic crude extract at 283 nm, and (b) Developed chromatoplate image of standard ergosterol with hydroalcoholic crude extract captured at 256 nm. | 66 |

| | |
|--|----|
| Figure 3.1. Graphical summary of BLAST analysis (a) pure culture, and (b) fresh mushroom of <i>P. osteratus</i> . | 77 |
| Figure 3.2. Morphological growth of <i>P. osteratus</i> . | 78 |
| Figure 3.3. Microscopic features of <i>P. osteratus</i> (a) Basidia (b) Basidiospores (c) Cheilocystidia (d) Generative hyphae showing clamp connections, and (e) Pleurocystidia scale bar (a-e) = 10µm. | 78 |
| Figure 3.4. Line drawings of microscopic features of <i>P. osteratus</i> (a) Basidia (b) Basidiospores (c) Generative hyphae showing clamp connections, and (d) Pleurocystidia scale bar (a-d) = 10µm. | 79 |
| Figure 3.5. <i>In-vitro</i> cytotoxic activity of PO1 and its fraction against MDA-MB-231 and A549. Non-linear regression analysis was performed for the determination of IC ₅₀ . Values are expressed as mean ± standard deviation (SD) of three parallel measurements. One-way ANOVA was performed, followed by a turkey's multiple comparison test using Graph pad prism 5.0. Different letters (a, b, c, and d) represent a significant difference at (p < 0.05), and the same letter indicates the absence of a significant difference between the results. | 80 |
| Figure 3.6. Heat-map representation (IC ₅₀) of PO1, HFPO1, and EFPO1 fraction against the panel of cancer cell lines. | 81 |
| Figure 3.7. Polyphenolic content of PO1, HFPO1, and EFPO1, with inset figure showing ergosterol content of PO1, HFPO1, and EFPO1. The value are expressed as mean ± standard deviation (SD). One-way ANOVA was performed followed by the turkey's multiple comparison test using Graph pad prism 5.0. *** Significance difference (p < 0.001), ** significance difference (p < 0.05), and * significance difference (p < 0.01). | 83 |
| Figure 3.8. Chromatogram of PO1, HFPO1, and EFPO1 (a) (b), and (c) Chromatogram of PO1, HFPO1, and EFPO1 in positive mode, respectively and (d) (e), and (f) Chromatogram of PO1, HFPO1, and EFPO1 in negative mode, respectively. | 85 |
| Figure 3.9. MS spectra of (a) D- pantothenic acid (b) acremoauxin A (c) carbendazim (d) cephaeline (e) asterosterol (f) ophiobolin F (g) betulin (h) 16,28-Secosolanidan-23-ol,3-amino-16,23-epoxy-, (3beta,5alpha,16alpha,22alpha,23beta,25beta)- (i) Senecionine (j) Cholest-5-ene (k) (3b,6b,8a,12a)-8,12-epoxy-7(11)-eremophilene-6,8,12-trimethoxy-3-ol (l) beta-obscurine (m) myxalamid B (n) avocadyne 1-acetate (o) avocadyne 4-acetate (p) momordol (q) (13R,14R)-7-Labdene-13,14,15-triol (r) linoleoyl ethanolamide (s) dihydroanhydorhodovibrine and (t) polyporusterone G. | 88 |
| Figure 3.10. Unsupervised chemometric analysis of PO1, HFPO1, and EFPO1 (a) Bi-plot of PCA analysis of identified myco-metabolites in PO1, HFPO1, and EFPO1; (b) Loading plot of PCA analysis of the identified myco-metabolites in PO1, HFPO1, and EFPO1; and (c) HCA dendrogram of identified myco-metabolites in PO1, HFPO1, and EFPO1. | 92 |
| Figure 3.11. Supervised chemometric analysis of PO1, HFPO1, and EFPO1 (a) 3-D view of loading plot of PLS analysis of identified myco-metabolites contributing to bioactivities, in PO1, HFPO1, and EFPO1; (b) Bi-plot of PLS analysis of the identified myco-metabolites contributing to bioactivities, in PO1, HFPO1, and EFPO1; and (c) VIP score of the identified myco-metabolites contributing to bioactivities, in PO1, HFPO1, and EFPO1. | 94 |

| | |
|---|-----|
| Figure 4.1. Methodology for <i>in-vivo</i> anti-tumor efficacy of HFPO1 in EAC (solid tumor) bearing Swiss albino mice. | 108 |
| Figure 4.2. Venn diagram of overlapping myco-metabolites-target genes (a) with Malacards database for BC, HC, and LC (b) with DisGeNet database for BC, HC and LC, and (c) altogether from MalaCards and DisGeNet database. | 120 |
| Figure 4.3. STRING protein-protein interaction of 74 target genes. | 121 |
| Figure 4.4. Protein-Protein interaction of 58 target genes. Yellow nodes represent the top 10 nodes based on degree. | 122 |
| Figure 4.5. Top 10 Gene ontology enrichment in three arenas (a) biological process (b) cellular component, and (c) molecular function of 58 target genes. | 125 |
| Figure 4.6. Dot plot of top 10 KEGG pathways of 58 target genes. | 126 |
| Figure 4.7. Target genes involved in KEGG's pathway of cancer. | 127 |
| Figure 4.8. Interaction between myco-metabolites of HFPO1 with 58 target genes and top 10 KEGG pathways. | 128 |
| Figure 4.9. Molecular docking analysis of HFPO1 myco-metabolites with their respective target gene (a) LIN and EGFR (PDB Id: 6LUD) (b) MOM and ESR1 (PDB Id: 6W0K) (c) MOM and JAK2 (PDB Id: 6VGL) (d) MOM and MAPK3 (PDB Id: 7M0Y) (e) LIN and CDK1 (PDB Id: 6GU6) (f) MOM and PIK3CA (PDB Id: 4JPS) (g) SOL and AKT1 (PDB Id: 4EKL). | 130 |
| Figure 4.10. <i>In-silico</i> cancer multi-omic expression study and prognostic potential of selected hub target (PI3KCA, and AKT1) for acute myeloid leukaemia (a) genomic expression, and (b) overall survival analysis. | 131 |
| Figure 4.11. Fluorescence micrographs (DAPI stained) of untreated and treated HL-60 cancer cell line with HFPO1 (0-200 µg/mL). Scale bar: 1µm; Magnification: 20X. | 133 |
| Figure 4.12. Immunoblot analysis using antibodies against P110α, AKT, and mTOR protein in HFPO1 treated HL-60 (0-200 µg/mL). | 134 |
| Figure 4.13. Histopathological examination of liver and kidney of HFPO1 (175 mg/kg) group against control Swiss albino mice group for acute toxicity assessment. Scale bar: 1µm; Magnification: 10X. | 136 |
| Figure 4.14. <i>In-vivo</i> anti-tumor efficacy in EAC (solid tumor) bearing Swiss albino mice. Values are expressed as Mean ± SD (n = 5). One-way ANOVA was performed, followed by the turkey's multiple comparison test (p < 0.05), using Graph pad prism 5.0. Different letters (a, b, and c) represent a significant difference at p < 0.05 & same letters represent absence of significant difference. | 138 |
| Figure 5.1. Venn diagram of overlapping myco-metabolites-target genes (a) with Malacards database for BC, HC, and LC (b) with DisGeNet database for BC, HC and LC, and (c) altogether from MalaCards and DisGeNet database. | 164 |
| Figure 5.2. Protein-Protein interaction of 90 target genes. Yellow nodes represent the top 10 nodes based on degree. | 165 |
| Figure 5.3. Top 10 Gene ontology enrichment in three arenas (a) biological process (b) cellular component, and (c) molecular function of 90 target genes. | 169 |
| Figure 5.4. Dot plot of top 10 KEGG pathways of 90 target genes. | 170 |
| Figure 5.5. Target genes involved in KEGG's pathway of cancer. | 171 |
| Figure 5.6. Interaction between myco-metabolites of EFPO1 with 90 target genes. | 172 |

| | |
|--|-----|
| Figure 5.7. Molecular docking analysis of EFPO1 myco-metabolites with their respective target gene (a) LUT and EGFR (PDB Id: 6LUD) (b) CEP and ESR1 (PDB Id: 6W0K) (c) CEP and MAPK3 (PDB Id: 7M0Y) (d) PA and BCL2L1 (PDB Id: 4LVT), and (e) KAM and AKT1 (PDB Id: 4EKL)..... | 174 |
| Figure 5.8. <i>In-silico</i> cancer multi-omic expression study and prognostic potential of selected hub target BCL2L1 in lung adenocarcinoma patients (a) genomic expression (b) proteomic expression, and (c) overall survival analysis. | 175 |
| Figure 5.9. Fluorescence micrographs (DAPI stained) of untreated and treated A549 cancer cell line with EFPO1 (0-200 µg/mL). Scale bar: 1µm; Magnification: 20X. | 176 |
| Figure 5.10. Immunoblot analysis using antibodies against BCL2L1, and BAX protein in EFPO1 treated A549 (0-200 µg/mL). | 177 |
| Figure 5.11. Histopathological examination of liver and kidney of EFPO1 (550 mg/kg) group against control Swiss albino mice group for acute toxicity assessment. Scale bar: 1µm; Magnification: 10X..... | 179 |
| Figure 5.12. <i>In-vivo</i> anti-tumor efficacy in EAC (solid tumor) bearing Swiss albino mice. Values are expressed as Mean ± SD (n = 5). One-way ANOVA was performed followed by the turkey's multiple comparison test (p < 0.05). Different letters (a, b, and c) represent a significant difference at p < 0.05 & same letters represent absence of significant difference..... | 181 |

List of Tables

| | |
|--|-----|
| Table 1.1. Reported anti-cancer potential of <i>Pleurotus</i> mushroom. | 30 |
| Table 2.1. Extraction yield of DCM: Et and hydroalcoholic crude extracts of different species of the <i>Pleurotus</i> mushroom. | 53 |
| Table 2.2. Total phenolic, flavonoids, carbohydrates, and protein contents in the DCM: Et and hydroalcoholic crude extracts of different species of <i>Pleurotus</i> mushroom. | 55 |
| Table 2.3. Calibration curve of standard ergosterol amount per spot versus mean peak area. | 65 |
| Table 2.4. Linear regression analysis of calibration curve and LOD and LOQ of standard ergosterol. | 65 |
| Table 2.5. Intra-day and inter-day precision of standard ergosterol (n = 3). | 65 |
| Table 2.6. Accuracy data of standard ergosterol (n = 3). | 66 |
| Table 3.1. Optimized MRM conditions for phenolic acids, flavonoids, and ergosterol estimation. | 73 |
| Table 3.2. Inference of BLAST analysis. | 76 |
| Table 3.3. LC-QTOF/MS- based tentative identified of myco-metabolites in PO1, HFPO1, and EFPO1 of <i>P. osteratus</i> | 89 |
| Table 4.1. Drug-likeness properties of tentatively identified myco-metabolites. | 109 |
| Table 4.2. List of the predicted targets for tentatively identified myco-metabolites. . | 110 |
| Table 4.3. Overlapped myco-metabolites-target genes with MalaCards diseases-target genes. | 113 |
| Table 4.4. Overlapped myco-metabolites-target genes with DisGeNet diseases-target genes. | 115 |
| Table 4.5. Topological analysis of protein-protein interaction of 58 target genes. | 122 |
| Table 4.6. Docking scores of hub target genes with their respective HFPO1 myco-metabolites. | 129 |
| Table 4.7. Biochemical parameters of HFPO1 (175 mg/kg) group against control Swiss albino mice for acute toxicity assessment. | 135 |
| Table 4.8. Hematological parameters of HFPO1 (175 mg/kg) group against control Swiss albino mice group for acute toxicity assessment. | 136 |
| Table 4.9. Change in weight (g) of HFPO1 (175 mg/kg) group in Swiss albino mice for acute toxicity assessment. | 136 |
| Table 4.10. Biochemical parameters of control group, tumor-bearing mice group (T), and treated group (H1, H2, H3, and S) of tumor-bearing mice. | 139 |
| Table 4.11. Change in weight (g) of the control group, tumor-bearing mice group (T), and treated group (H1, H2, H3, and S) of tumor-bearing mice. | 139 |
| Table 5.1. Drug-likeness properties of tentatively identified myco-metabolites. | 152 |
| Table 5.2. List of the predicted targets for quantified and tentatively identified myco-metabolites. | 153 |
| Table 5.3. Overlapped myco-metabolites-target genes with MalaCards diseases-target genes. | 156 |
| Table 5.4. Overlapped myco-metabolites-target genes with DisGeNet diseases-target genes. | 159 |

| | |
|---|-----|
| Table 5.5. Topological analysis of protein-protein interaction of 90 target genes. | 166 |
| Table 5.6. Docking scores of hub target genes with their respective EFPO1 myco-metabolites..... | 173 |
| Table 5.7. Biochemical parameters of EFPO1 (550 mg/kg) group against control Swiss albino mice for acute toxicity assessment. | 178 |
| Table 5.8. Hematological parameters of EFPO1 (550 mg/kg) group against control Swiss albino mice group for acute toxicity assessment. | 179 |
| Table 5.9 Change in weight (g) of EFPO1 (550 mg/kg) group in Swiss albino mice for acute toxicity assessment..... | 179 |
| Table 5.10. Biochemical parameters of control group, tumor-bearing mice group (T), and treated group (E1, E2, E3, and S) of tumor-bearing mice. | 182 |
| Table 5.11. Change in weight (g) of control group, tumor-bearing mice group (T), and treated group (E1, E2, E3, and S) of tumor-bearing mice..... | 182 |

List of Equations

| | |
|-------------------|-----|
| Equation 2.1..... | 47 |
| Equation 2.2..... | 49 |
| Equation 2.3..... | 50 |
| Equation 4.1..... | 106 |

Symbols

| | |
|------------------|----------------------------------|
| °C | Degree Celsius |
| nm | Nanometre |
| µm | Micrometre |
| mm | Millimetre |
| cm | Centimetre |
| µL | Microliter |
| mL | Milliliter |
| g | Gram |
| µg | Microgram |
| kg | Kilogram |
| mM | Millimolar |
| M | Molar |
| % | Percentage |
| min | Minutes |
| sec | Seconds |
| v/v | Volume per volume |
| w/w | Weight per weight |
| vs | Versus |
| ± | Plus minus |
| < | Less than |
| λ _{max} | Wavelength at maximum absorbance |
| a.u. | Absorbance unit |
| R _f | Retention factor |
| R _t | Retention time |
| m/z | Mass-to-charge ratio |

Abbreviation

| | |
|---------|--|
| ABTS | 2,2'-azino-bis(3-ethylbenzothiazoline-6-sulfonic acid) |
| ACR | Acremoauxin A |
| AFPO1 | Aqueous of DCM: Et crude extract of <i>Pleurotus osteratus</i> |
| ANOVA | Analysis of Variance |
| API | Apigenin |
| AST | Asterosterol |
| AVO1 | Avocadyne 1-acetate |
| AVO4 | Avocadyne 4-acetate |
| | |
| BET | Betulin |
| BFPO1 | Butanol of DCM: Et crude extract of <i>Pleurotus osteratus</i> |
| BSA | Bovine serum albumin |
| | |
| CAR | Carbendazim |
| CEP | Cephaeline |
| CGA | Chlorogenic acid |
| CHOL | Cholest-5-ene |
| COUA | p-coumaric acid |
| | |
| DCM:Et | 1:1 v/v dichloromethane: ethanol |
| DMEM | Dulbecco's Modified Eagle Medium |
| DPPH | 2,2-Diphenyl-1-picrylhydrazyl |
| | |
| EFPO1 | Ethyl acetate of DCM: Et crude extract of <i>Pleurotus osteratus</i> |
| ERE | (3b,6b,8a,12a)-8,12-epoxy-7(11)-eremophilene-6,8,12-trimethoxy-3-ol |
| ERG | Ergosterol |
| | |
| FBS | Fetal bovine serum |
| | |
| GC-HS | Headspace gas chromatography |
| GEPIA 2 | Gene Expression Profiling Interactive Analysis 2 |

| | |
|------------------|---|
| GO | Gene Ontology |
| HCA | Hierarchical Cluster Analysis |
| HFPO1 | Hexane of DCM: Et crude extract of <i>Pleurotus osteratus</i> |
| HPTLC | High-performance thin-layer chromatography |
| IC ₅₀ | Half maximal inhibitory concentration |
| KAM | Kaempferol |
| KEGG | Kyoto Encyclopedia of Genes and Genomes |
| LAB | (13R,14R)-7-Labdene-13,14,15-triol |
| LC-MS/MS | Liquid Chromatography with tandem mass spectrometry |
| LD ₅₀ | Median lethal dose |
| LIN | Linoleoyl ethanolamide |
| LOD | Limit of detection |
| LOQ | Limit of quantification |
| LUT | Luteolin |
| MOM | Momordol |
| MTT | 3-[4,5-dimethylthiazol-2-yl]-2,5 diphenyl tetrazolium bromide |
| MYX | Myxalamid B |
| NA | Naringenin |
| OBS | Beta-obscurine |
| OPH | Ophiobolin F |
| PA | Protocatechuic acid |
| PAN | D- pantothenic acid |
| PCA | Principal component analysis |
| PD1 | DCM: Et crude extract of <i>Pleurotus roseus</i> |
| PD2 | Hydroalcoholic crude extract of <i>Pleurotus roseus</i> |

| | |
|--------|--|
| PE1 | DCM: Et crude extract of <i>Pleurotus eryngii</i> |
| PE2 | Hydroalcoholic crude extract of <i>Pleurotus eryngii</i> |
| PF1 | DCM: Et crude extract of <i>Pleurotus florida</i> |
| PF2 | Hydroalcoholic crude extract of <i>Pleurotus florida</i> |
| PLS | Partial least square |
| p.o. | Per oral |
| PO1 | DCM: Et crude extract of <i>Pleurotus osteratus</i> |
| PO2 | Hydroalcoholic crude extract of <i>Pleurotus osteratus</i> |
| POL | Polyporusterone G |
| PPI | Protein-protein interaction |
| PS1 | DCM: Et crude extract of <i>Pleurotus sajor caju</i> |
| PS2 | Hydroalcoholic crude extract of <i>Pleurotus sajor caju</i> |
| RHOD | Dihydroanhydorrhodovibrine |
| RPM | Rotation per minute |
| s.c. | Subcutaneous |
| SD | Standard deviation |
| SE | Standard error |
| SEN | Senecionine |
| SOL | 16,28-Secosolanidan-23-ol,3-amino-16,23-epoxy-, (3beta,5alpha,16alpha,22alpha,23beta,25beta)- |
| STRING | Search Tool for the Retrieval of Interacting Genes/Proteins |
| UALCAN | University of ALabama at Birmingham CANcer data analysis Portal |

Preface

Pleurotus osteratus (*P. osteratus*), a species from the *Pleurotus* genus, has been intensively studied for its anti-cancer activity, attributed to higher molecular weight myco-metabolites. Conversely, little is known about the anti-cancer bioactivities associated with lower molecular weight myco-metabolites, to list a few ergosterols, and polyphenolic compounds claimed as lower molecular weight biomarkers responsible for anti-cancer activities of *P. osteratus*. Besides this, the comprehensive myco-metabolite profiling, the correlation between myco-metabolites and their bioactivities, and underlying mechanisms are still illusive.

The presented research work was designed to explore differential bioactivity-based screening of preferential extracted higher molecular weight, and lower molecular weight myco-metabolites, a detailed myco-metabolite profiling, and correlating with bioactivity and tracing mechanistic pathway involved in the anti-cancer intervention of potential one.

The thesis is divided into six chapters and are as follows:

Chapter 1 deals with the exhaustive review on explored anti-cancer potential of *Pleurotus* mushroom till date, an overview on chemometric and network pharmacology, and along with rationale and research objectives. **Chapter 2** explores the bioactivity-based screening of different species of *Pleurotus* mushroom with their myco-chemical profiling. **Chapter 3** describes chemometric-based analysis of myco-metabolite of bioactive enriched fraction of *Pleurotus osteratus* (screened species) and its correlation with in-vitro cytotoxic activity. **Chapter 4** presents tracing the anti-cancer mechanism of HFPO1 (potential fractionate of *P. osteratus*) by the integrative approach of network pharmacology and experimental studies.

Chapter 5 documents tracing the anti-cancer mechanism of EFPO1 (potential fractionate of *P. osteratus*) by the integrative approach of network pharmacology and experimental studies. **Chapter 6** represents the overall summary and conclusion of the research work.